Shahid Beheshti University

Sustainable Earth Trends

Journal homepage: http://sustainearth.sbu.ac.ir

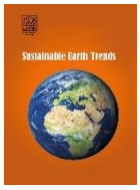

Spatial assessment of soil erosion using the RUSLE model and remote sensing data processed in google earth engine: A case study of the Birjand plain

Amir Khazaei[a*], Fatemeh Sahragard[b], Elham Yousefi[b]

[a] Department of Water Science and Engineering, Faculty of Agriculture, University of Birjand, Birjand, Iran
[b] Department of Environmental Engineering, Faculty of Natural Resources and Environment, University of Birjand, Birjand, Iran

ABSTRACT

Soil erosion is a major environmental challenge in arid and semi-arid regions, threatening agricultural productivity, water resources, and ecological stability. This study quantified and spatially analyzed soil erosion in the Birjand Plain, eastern Iran, by integrating the Revised Universal Soil Loss Equation (RUSLE) model with satellite-derived data using the Google Earth Engine (GEE) cloud-computing platform. Key erosion factors—including rainfall erosivity (R), soil erodibility (K), slope length and steepness (LS), cover management (C), and support practices (P)—were extracted from multi-source remote sensing datasets. The results revealed considerable spatial variability in erosion intensity across the plain. Approximately 67.3% of the area experiences very low soil loss rates (0–10 tons/ha/year), while 22.9% is categorized as low erosion (10–20 tons/ha/year). Moderate (20–40 t/ha/year), high (40–60 t/ha/year), and very high (>60 t/ha/year) erosion zones constitute 7.5%, 2.0%, and 0.2% of the area, respectively. These high-risk zones are often associated with steep terrain, sparse vegetation, and poor land management. The use of GEE facilitated fast, large-scale erosion modeling with high spatial resolution and minimal reliance on ground data. This approach proves to be scalable, cost-efficient, and reproducible, particularly for data-scarce regions. The findings provide valuable insights for land managers and policymakers aiming to prioritize soil conservation efforts and develop sustainable land-use strategies. This research underscores the potential of integrating remote sensing and cloud-based tools with empirical models to enhance environmental monitoring and resilience in erosion-prone landscapes.

ARTICLE INFO

Keywords:
Birjand Plain
Google Earth Engine
Soil erosion
Sustainable land management
Remote sensing

Article history:
Received: 02 July 2025
Accepted: 14 August 2025

*Corresponding author
E-mail address:
amir.khazaei@birjand.ac.ir
(A. Khazaei)

Citation:
Khazaei, A. et al., (2026). Spatial assessment of soil erosion using the RUSLE model and remote sensing data processed in google earth engine: A case study of the Birjand plain, *Sustainable Earth Trends:* 6(3), (20-34).

DOI: 10.48308/set.2025.240705.1139

1. Introduction

Soil erosion is recognized as one of the most critical and widespread environmental issues worldwide, with severe impacts on natural resources, agricultural productivity, and ecological balance (Pimentel, 2006; Owens and Collins, 2006; Robinson et al., 2017). The increasing intensity of human activities, such as unsustainable agriculture, overgrazing, and deforestation, has accelerated the process of soil degradation (Chuenchum et al., 2020). This phenomenon reduces soil fertility and weakens the agricultural productivity of the land. It also contributes to vegetation degradation, increases the risk of water pollution and salinization, and elevates the likelihood of floods. Moreover, it can damage infrastructure and reduce both the storage capacity and operational lifespan of dams and reservoirs (Oveisi et al., 2015; Ebrahimzadeh et al., 2018). Soil erosion has dramatically intensified in the 20th century and is projected to worsen in some parts of the world due to the impacts of climate change (Panagos et al., 2010; Asadi et al., 2017). Among all continents, Asia is the most affected, and Iran is among the countries with the highest soil erosion rates in this region. The average soil erosion rate in Iran is approximately 25 tons per hectare per year, which is more than 4.3 times the global average (Rostamian et al., 2008). However, proper soil management can significantly

enhance food security, carbon storage, and ecosystem sustainability (Le Roux et al., 2008). In response to this growing concern, numerous studies have been conducted to develop effective soil management policies at both regional and national levels (Guerra et al., 2016; Wang and Su, 2020; Xu et al., 2020). A sound understanding of the spatial and temporal dynamics of soil erosion is essential for designing effective scientific and practical erosion control strategies (Tamene et al., 2017; Alewell et al., 2019). In recent decades, predicting soil erosion intensity at regional scales has become a major environmental challenge (Biddoccu et al., 2020). To address this, several models have been developed, including SEMMED (De Jong et al., 1999), WEPP (Boardman et al., 2006), SWAT (Neitsch et al., 2011), USPED (Mitasova et al., 1996), InVEST (Natural Capital Project, 2022), and TerrSet (Clark Labs, 2022). Among them, the Revised Universal Soil Loss Equation (RUSLE) has been widely used in large-scale studies due to its relatively simple structure, reasonable accuracy, and compatibility with Remote Sensing (RS) and Geographic Information Systems (GIS) technologies (Farhan and Nawaiseh, 2015; Behera et al., 2020).

Although RUSLE was initially developed using data from the United States, numerous studies have since examined the adaptability of its parameters in diverse climatic conditions, complex topographies, land use types, and soil characteristics (Duan et al., 2020; Kebede et al., 2020). Notably, USLE and its revised version, RUSLE, remain the most commonly used models for estimating soil erosion and sediment yield in watersheds. Nevertheless, limitations such as lack of real-time monitoring, restricted spatial coverage, and poor integration with water resource management systems can reduce the effectiveness of models like RUSLE and tools such as TerrSet. Therefore, integrating advanced models with modern information technologies offers a promising approach for enhancing the accuracy and efficiency of soil erosion modeling (Walker and Steffen, 1997; Belnap et al., 2011).

A growing number of studies in Iran have utilized RUSLE combined with remote sensing to evaluate erosion dynamics. For instance, Ghahremani et al. (2025) evaluated the impact of biological watershed management practices on erosion in the Chikan and Morzian basins between 1992 and 2021. Their findings revealed a reduction in average soil loss from 19.20 to 18.82 tons/ha/year. Gholami et al. (2024) assessed land use change effects on erosion in the Cherdawol watershed, showing an increase from 13.23 to 20.13 tons/ha/year, mainly driven by conversion of bare lands. Similarly, Garshasbi and Jokar (2024) found that deforestation and pasture loss between 1980–2020 in the Avard-Nakarood basin led to increased erosion from 1.64 to 1.75 tons/ha/year. Asghari and Babaei (2024) observed that reductions in farmland and increases in built-up areas in the Shafarood basin raised erosion rates from 5.63 to 8.37 tons/ha/year.

In addition, Jokar Sarhangi and Dehghan Chachkami (2022) compared RUSLE and ICONA models in mapping soil erosion severity in the Baladeh basin, reporting better accuracy for ICONA based on RMSE, MAE, and NSEC indicators. Gholami et al. (2024) also found that RUSLE provided acceptable estimates using either traditional or digital datasets and that slope-based models gave the most accurate SDR estimates. Terefe et al. (2024) confirmed the adaptability of RUSLE in Ethiopia, although they emphasized the need for better validation and precise inputs. Their reported erosion rates ranged from 12.94 to 576 tons/ha/year. Samarinas et al. (2024) integrated AI and satellite imagery to refine RUSLE outputs, revealing annual erosion of 1.76 tons/ha, particularly in mountainous zones.

These findings highlight a common theme: while the RUSLE model is effective and widely used, combining it with cutting-edge platforms like Google Earth Engine (GEE) can overcome its traditional limitations. GEE enables large-scale, cloud-based data processing and high-resolution spatiotemporal analysis without the need for extensive fieldwork. This provides new opportunities for efficient soil erosion monitoring, especially in arid and semi-arid regions.

Given the pressing issue of soil erosion in dry regions such as the Birjand plain, this study aims to estimate soil loss using the RUSLE model within the GEE environment. The use of cloud computing, enhanced temporal and spatial resolution, and reduced dependence on extensive field data represent the key innovations of this research. By integrating RUSLE with advanced remote sensing data on a cloud-based platform, we offer a fast and

spatially accurate erosion assessment at a regional scale. The use of cloud computing, enhanced temporal and spatial resolution, and reduced dependence on extensive field data represent the key innovations of this research. Moreover, by focusing on the Birjand plain—an area particularly vulnerable due to its dry climate—this study not only deepens scientific understanding but also provides a valuable framework for similar regions facing land degradation challenges.

2. Material and methods

2.1. Study area

The Birjand watershed, covering an area of approximately 3,455 km², comprises about 1,045 km² of plains and the remaining portion consists of mountainous terrain (Fig. 1). This region is located in an arid to semi-arid climate zone and exhibits significant topographic diversity. The highest elevation is Mount Bagh-e-Ran at 2,787 meters above sea level, while the lowest point is the village of Fadashk at 1,240 meters. The general slope of the land decreases from east to west. The average annual precipitation in the basin is approximately 156.7 mm, and the mean annual temperature is around 16.4°C. The Shahroud River originates in the eastern highlands, traverses 108 km while joining several tributaries, and eventually flows into the central plain and the Lut Desert. It plays a critical role in the hydrological system and water resource supply of the region (Rahimzadeh Kivi et al., 2015).

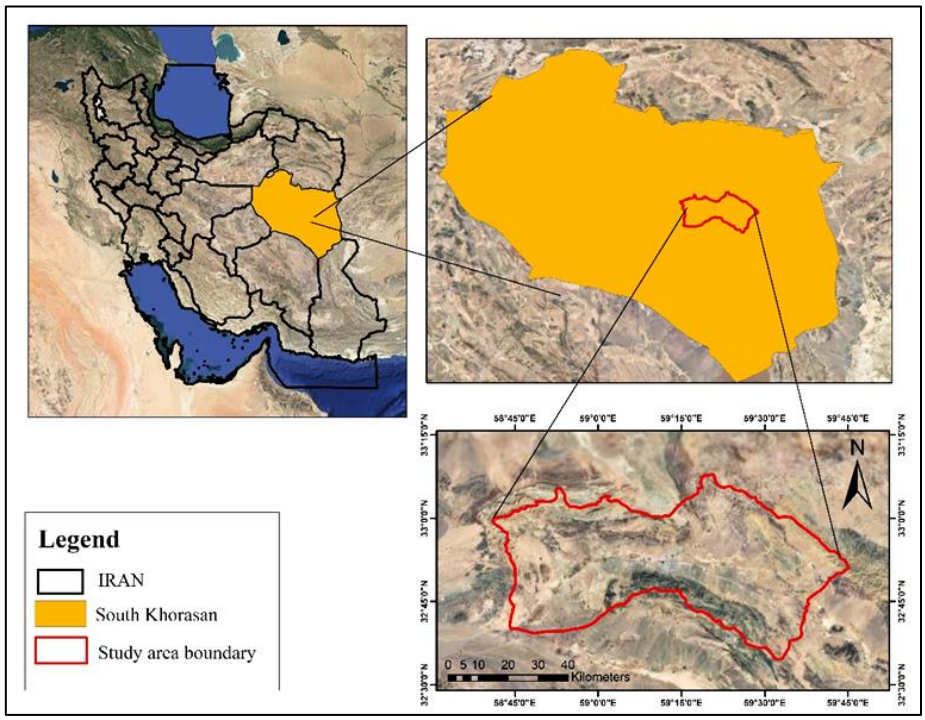

Fig. 1. Map of the study area.

The Revised Universal Soil Loss Equation (RUSLE) is an empirical model developed to estimate long-term average annual soil loss resulting from sheet and rill erosion. This model is especially applicable in regions characterized by specific slope conditions, land use types, and management practices (Renard et al., 1997; Wischmeier and Smith, 1978; Sonneveld and Nearing, 2003). The general form of the RUSLE model is as Eq. 1:

$$A = R \times K \times LS \times C \times P \qquad (1)$$

Where:

- **A**: Estimated average annual soil loss (tons·ha^{-1}·yr^{-1})
- **R**: Rainfall-runoff erosivity factor (MJ·mm·ha^{-1}·h^{-1}·yr^{-1})
- **K**: Soil erodibility factor (tons·hour / MJ·mm)
- **LS**: Topographic factor (slope length and steepness; dimensionless)
- **C**: Cover-management factor (dimensionless)
- **P**: Support practice factor (dimensionless)

RUSLE has been widely employed in natural resource studies, particularly for watershed-scale conservation planning. Its adaptability and simplicity make it suitable for integration with GIS and remote sensing tools in order to analyze spatial patterns of soil erosion and to support the development of soil conservation strategies.

2.2. Rainfall erosivity factor (R)

The monthly rainfall erosivity factor (R) was calculated using Eq. 2, as proposed by Wischmeier and Smith (1978). This equation estimates the potential of rainfall to cause soil erosion. A higher R value indicates a greater erosive impact of precipitation on the soil in a given region.

$$R = 1.73 * 10^{\left(1.5*\mathrm{LOG}\left(\frac{P_M^2}{P_A}\right)-0.08188\right)} \quad (2)$$

Where:

- **R**: Rainfall erosivity ($MJ \cdot mm \cdot ha^{-1} \cdot h^{-1} \cdot yr^{-1}$)
- **Pm**: Monthly precipitation (mm)
- **Pa**: Annual precipitation (mm)

In this study, monthly precipitation data in millimeters were obtained with a spatial resolution of 1 km, using a combination of datasets including SM2RAIN-ASCAT (2007–2019), IMERG, CHELSA climate data, and WorldClim. These datasets were spatially downscaled to 1 km resolution using the gdalwarp tool with a cubic spline interpolation method. For each month, the average value from WorldClim, CHELSA, and IMERG was computed and used in the calculation. The SM2RAIN-ASCAT dataset, due to its higher accuracy, was assigned a weight three times greater than the others to ensure greater influence in the final precipitation composite. The full data processing workflow is documented and available in the respective data source. Monthly precipitation values for each pixel, ranging from 0 to 380 mm, were generated in raster format for all months from January to December.

2.3. Soil erodibility factor (K)

This factor represents the susceptibility of soil particles to detachment and transport by rainfall and surface runoff. In this study, the K factor was computed using a complex empirical formula incorporating exponential and trigonometric functions, based on the percentage of sand (m_s), silt (m_silt), clay (m_c), and organic carbon content (org_C). The equation provides a more precise estimation of soil erodibility by considering the interactions between soil texture and organic matter (Eq. 3).

$$\begin{aligned} K &= \left\{0.2 + 0.3\exp\left[-0.0256 m_s \left(1 - \frac{m_{silt}}{100}\right)\right]\right\} \times \left[\frac{m_{silt}}{m_c + m_{silt}}\right]^{0.3} \\ &\times \left\{1 - \frac{0.25\ \mathrm{org\ C}}{[\mathrm{org\ C} + \exp(3.72 - 2.95\mathrm{org\ C})]}\right\} \\ &\times \left\{1 - \frac{0.7\left(1 - \frac{m_s}{100}\right)}{\left\{\left(1 - \frac{m_s}{100}\right)\exp\left[-5.51 + 22.9\left(1 - \frac{m_s}{100}\right)\right]\right\}}\right\} \end{aligned} \quad (3)$$

Where:

- **m_s**: Percentage of sand (%)
- **m_silt**: Percentage of silt (%)
- **m_c**: Percentage of clay (%)
- **org_C**: Organic carbon content (%)

2.4. Sand content (m_s)

This dataset, provided by *EnvirometriX Ltd*, includes sand fraction data for six standard soil depths (0, 10, 30, 60, 100, and 200 cm) at a 250-meter spatial resolution. Among the six available standard soil depths, the B0 layer (0 cm) was selected for this analysis, since surface soil properties have the most direct influence on erosion susceptibility in RUSLE modeling. The data, covering the period from 1950 to 2018, were generated using machine learning algorithms trained on global soil sample databases. Antarctica is excluded from this dataset. The maps are accessible via the Google Earth Engine (GEE) platform.

2.5. Clay content (m_c)

Also supplied by *EnvirometriX Ltd*, this dataset provides clay content across the same six standard depths and spatial resolution (250 m), and is based on the same time period (1950–2018). For this study, only the B0 depth layer (0 cm) was used, as it best represents the surface soil conditions relevant to erosion modeling. The data were modeled using machine learning algorithms on a global soil profile database. All data processing steps are well-documented, and the dataset is accessible via GEE.

2.6. Soil Organic carbon content (org_C)

This dataset, titled *Soil Organic Carbon Content*, is likewise provided by *EnvirometriX Ltd* and is accessible through GEE. It reports organic carbon content in units of 5 g/kg for six depths (0–200 cm) with a 250-meter spatial

resolution. The analysis was based on the surface layer (0 cm), considering that organic carbon content in topsoil plays a crucial role in determining soil structure and susceptibility to erosion. Like the previous datasets, it was generated using predictions based on a global compilation of soil point data. Antarctica is excluded, and full metadata are available through OpenLandMap documentation.

2.7. Silt content (m_silt)

Silt percentages were estimated based on the Soil Texture Classes dataset from OpenLandMap, using the USDA classification system. This dataset was also developed by EnvirometriX Ltd for the period 1950–2018 and made available on GEE with 250-meter resolution across six standard soil depths. To extract silt content, the soil texture class layer was downloaded from GEE and imported into ArcMap. Using the USDA soil texture triangle, silt percentages for each texture class were assigned. An Inverse Distance Weighting (IDW) interpolation was then applied to create a continuous spatial map of silt distribution. This method, based on the spatial autocorrelation principle, estimates silt content at unsampled locations by weighting the values of nearby known points. The resulting map provides valuable input for soil science, agricultural planning, and natural resource management. Among various interpolation methods evaluated, IDW was selected due to its computational efficiency, ease of implementation, and ability to effectively capture local spatial variations in silt content within the study area.

2.8. Slope length factor (LS)

The LS factor, representing the combined effects of slope length and steepness on soil erosion, was calculated using Eq. 4. This factor acts as an accelerator in rainfall-induced erosion processes. The slope length method was developed by Moore and Wilson (1992) and evaluated through stepwise coupling techniques (Liu et al., 1994; McCool et al., 1985):

$$LS = (0.4 + 1) \times (\text{Flowacc} \times \frac{\text{Cellsize}}{22.13})^{0.4} \times (\sin\theta / 0.0896)^{1.3} \quad (4)$$

Where:

- **LS**: horizontal slope length factor,
- **Flowacc**: flow accumulation (number of upstream cells contributing flow),
- **Cellsize**: spatial resolution of the DEM cells,
- **θ**: slope angle derived from the DEM.

Flow accumulation maps were generated using HydroSHEDS data collected between February 11 and 22, 2000. This dataset, provided by the World-Wide Fund for Nature (WWF), includes layers such as flow direction, flow accumulation, and a corrected Digital Elevation Model (DEM). It is based on NASA's Shuttle Radar Topography Mission (SRTM) data, with a spatial resolution of 15 arc-seconds (~463.83 m). Each pixel value in the flow accumulation layer (band b1) represents the number of upstream contributing cells, ranging from 1 to approximately 27.8 million. The dataset's accuracy decreases above 60°N latitude due to limited SRTM coverage.

2.9. Digital elevation model (DEM)

For DEM preparation, version 3 of the Shuttle Radar Topography Mission (SRTM) data was employed, provided by NASA, USGS, and JPL-Caltech, covering February 11–22, 2000. This DEM has a spatial resolution of 1 arc-second (~30 m) and includes gap-filling using open-source data such as ASTER GDEM2, GMTED2010, and NED. The elevation band records ground elevation in meters, ranging from -10 to 6500 m, and is widely used for topographical, hydrological, and surface modeling studies.

2.10. Vegetation cover factor (C)

The cover management factor (C) was calculated using the Normalized Difference Vegetation Index (NDVI), defined by Eq. 5:

$$\text{NDVI} = \frac{(\text{NIR} - \text{Red})}{(\text{NIR} + \text{Red})} \quad (5)$$

Where Red and NIR represent the reflectance values of red and near-infrared bands of electromagnetic radiation. The C factor was then derived by Eq. 6 based on NDVI and tropical climate conditions (Almagro et al., 2019):

$$C_{rA} = 0.1 \times \frac{(-\text{NDVI} + 1)}{2} \quad (6)$$

MODIS Terra mission data (MOD13Q1 version 6.1) were used to analyze vegetation

indices. These datasets, provided by NASA LP DAAC via USGS EROS, span from February 18, 2000, to April 7, 2025, with a 16-day revisit period and 250 m spatial resolution. The product contains two main vegetation indices: NDVI (measuring vegetation cover) and EVI (Enhanced Vegetation Index), which reduces background and atmospheric effects, especially in dense vegetation. Atmospheric corrected surface reflectance data were used, with water, cloud, smoke, and cloud shadow areas masked.

2.11. Support practice factor (P)

The support practice factor (P) is defined as the ratio of soil loss with a specific conservation practice to soil loss from up-and-down slope farming (Wischmeier and Smith, 1978). The resulting map was used to analyze conservation practices in the study area. The P factor ranges from 0 to 1, where values near 0 indicate high conservation efficiency and values near 1 represent low effectiveness. The empirical equation proposed by Weiner (1981), based on slope steepness (S), was used Eq. 7:

$$P = 0.2 + 0.03 \times S \qquad (7)$$

Land cover data from MODIS Terra and Aqua missions (MCD12Q1 version 6.1), provided by NASA LP DAAC via USGS EROS, were utilized to estimate P. This dataset includes annual land cover classifications with 500 m spatial resolution for 2001–2023, generated through supervised machine learning combining multiple classification systems (IGBP, FAO LCCS). Slope maps of the area were integrated to enhance P factor accuracy. The combination of these datasets provided a comprehensive estimation of support practice effects in hydrological modeling. The overall methodology and workflow of the calculations are illustrated in the flowchart presented in Fig. 2.

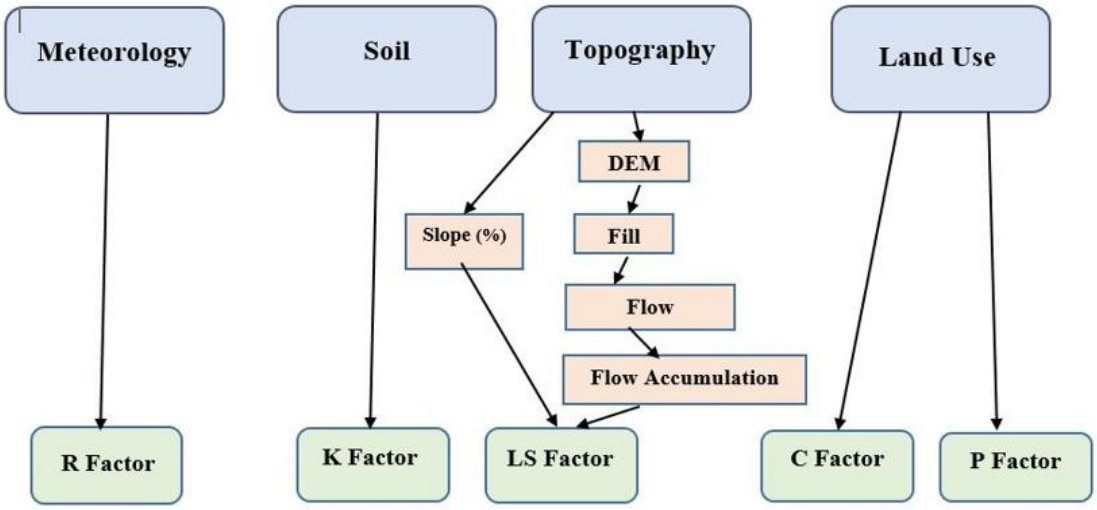

Fig. 2. RUSLE model implementation steps for soil erosion assessment.

3. Results and discussion

3.1. R factor

To calculate the R factor, the required data, including the intensity and annual rainfall pattern, were obtained from the Google Earth Engine data catalog. Using Eq .2, the annual rainfall erosivity factor (R) was computed. This factor represents the potential of rainfall to cause soil erosion and is expressed in megajoules millimeters per hectare per year (MJ·mm·ha^{-1}·yr^{-1}). Higher R values indicate a greater erosive potential of rainfall in the region. Based on the map extracted from Google Earth Engine, the R factor in the Birjand plain ranges from 112 to 227 MJ·mm/ha·h·yr. In Fig. 3, darker areas represent higher values, indicating that rainfall in those regions has a greater erosive impact on the soil. As this value increases, the risk of rainfall-induced soil erosion also rises.

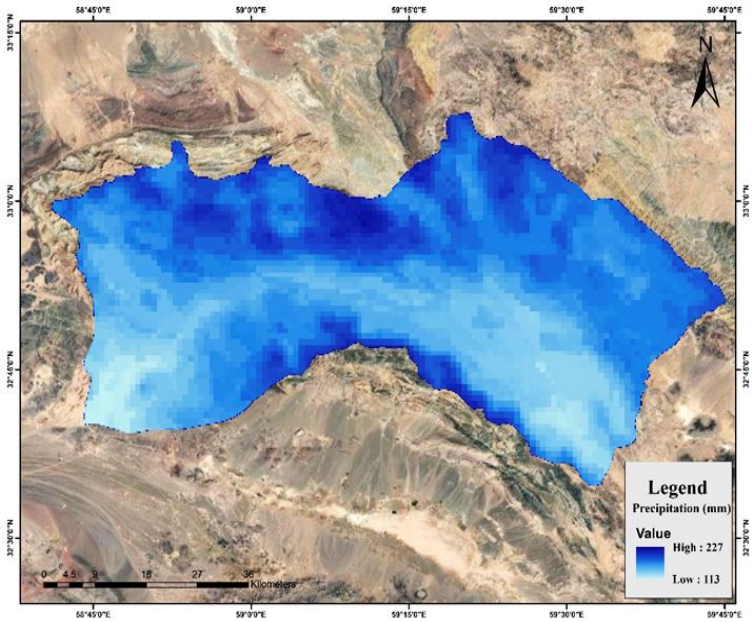

Fig. 3. Map of the rainfall erosivity factor (r) in the Birjand plain.

3.2. K factor

To calculate the soil erodibility factor (K), four variables are required: the percentage of sand, silt, clay, and soil organic carbon. The data for sand, silt, and clay percentages were obtained from the Google Earth Engine data catalog. Additionally, the silt percentage was extracted using interpolation methods in GIS software (Fig. 4).

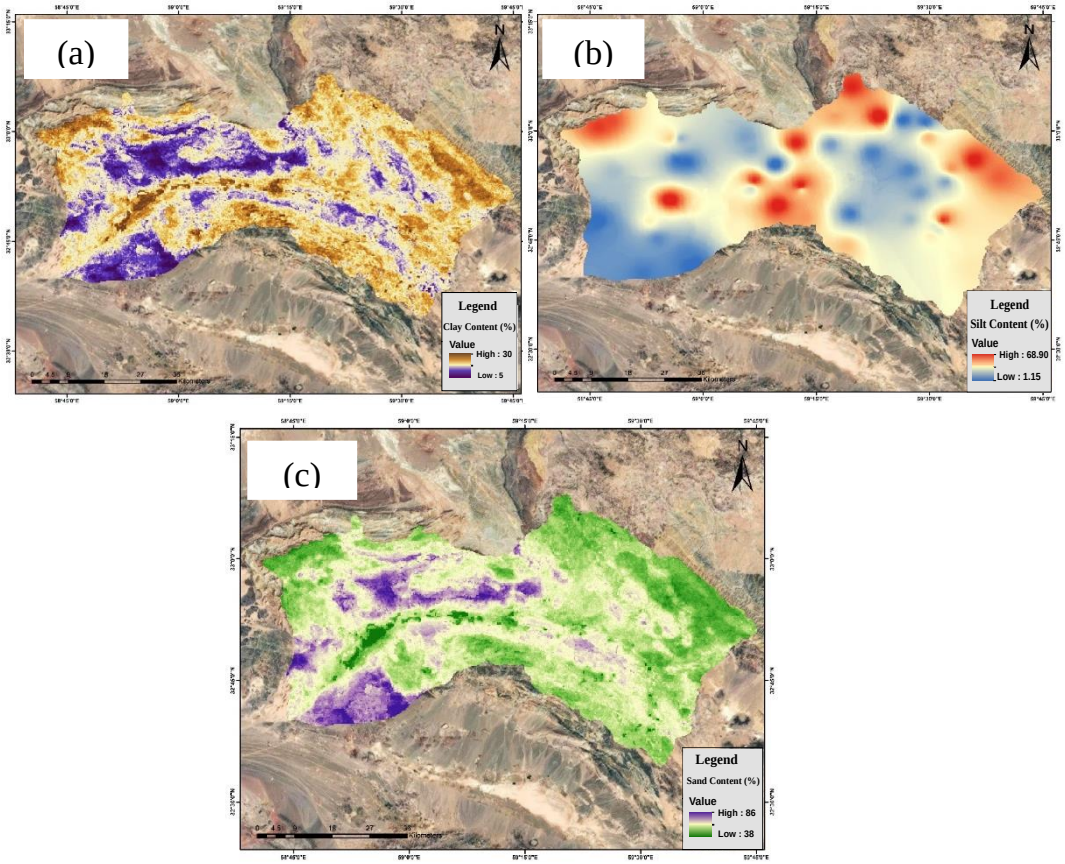

Fig. 4. Spatial distribution of the weight percentage of soil particles in the study area: (a) clay, (b) silt, and (c) sand, extracted from Google Earth Engine data.

Subsequently, based on the standard formula for calculating the K factor, the corresponding code was written and executed in Google Earth Engine to derive the values of the soil erodibility factor (K). These values ranged between 0.1 and 0.37 (ton·ha·h per MJ·mm). As shown in Fig. 5, higher K factor values indicate a greater susceptibility of soil to erosion. In other words, soils with higher K values are more vulnerable to the erosive effects of rainfall and surface runoff and tend to erode more rapidly.

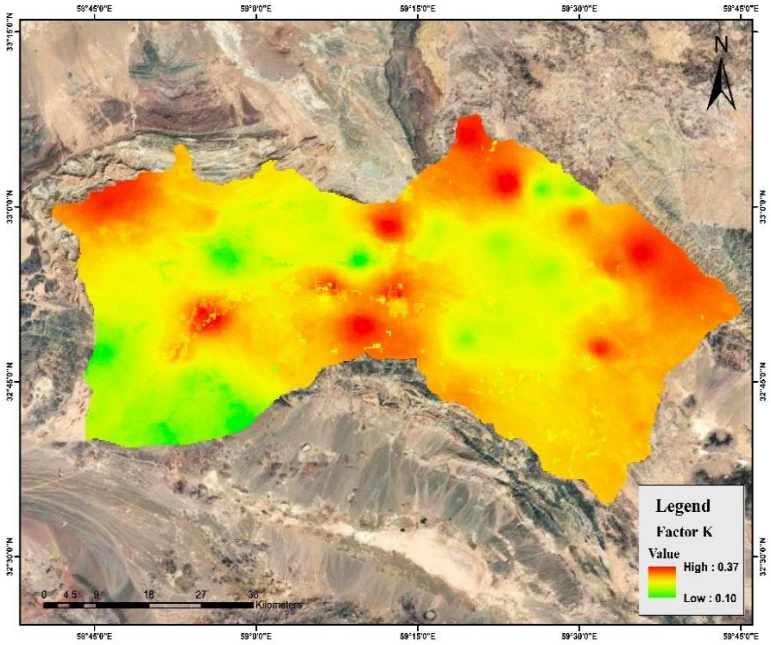

Fig. 5. Spatial distribution map of soil erodibility factor (K-factor) in the study area.

3.3. LS factor

To calculate the LS factor, flow accumulation data were obtained from the WWF HydroSHEDS map (unit: number of upstream pixels; higher values indicate main flow paths and greater water concentration), and slope data were extracted from Google Earth Engine (unit: percent; higher values reflect steeper slopes and higher erosion potential). These were retrieved as raster layers (Fig. 6). Using the standard equation, the corresponding code was implemented in Google Earth Engine to generate the LS factor map (Fig. 7). Higher LS values indicate increased erosion potential due to slope steepness and slope length.

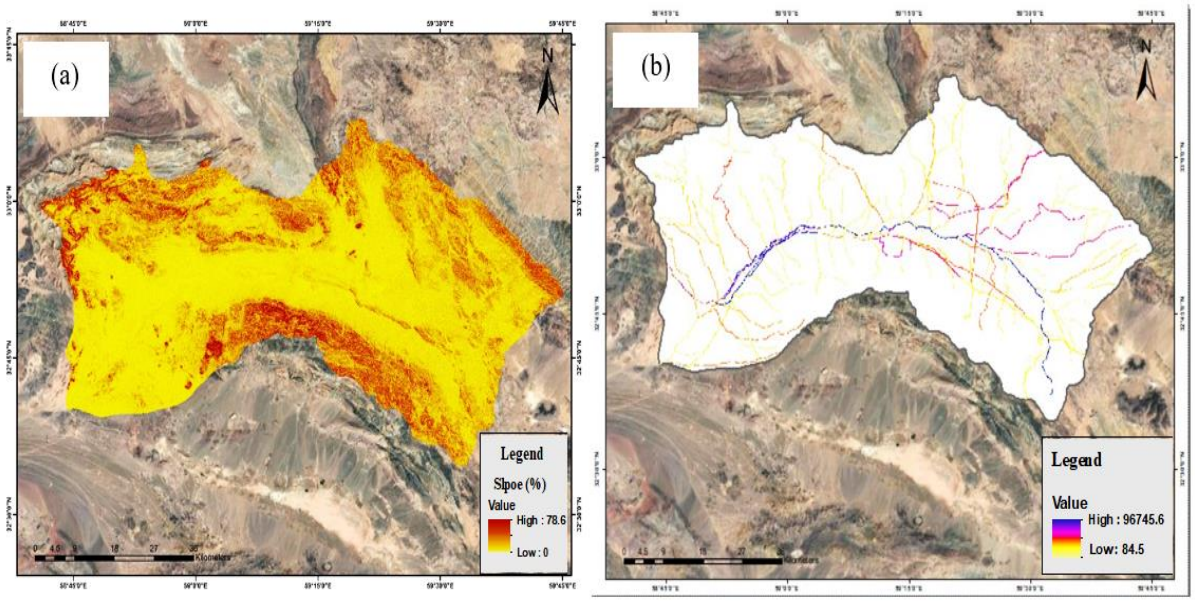

Fig. 6. (a) Slope map of the study area; (b) Flow accumulation map.

Subsequently, the flow accumulation and slope data were extracted from Google Earth Engine. Using well-established empirical relationships, a computational code was implemented in the Google Earth Engine environment to generate the LS factor map. Higher LS values indicate steeper slopes and longer flow paths, reflecting a greater potential for soil erosion due to the combined effect of slope gradient and slope length.

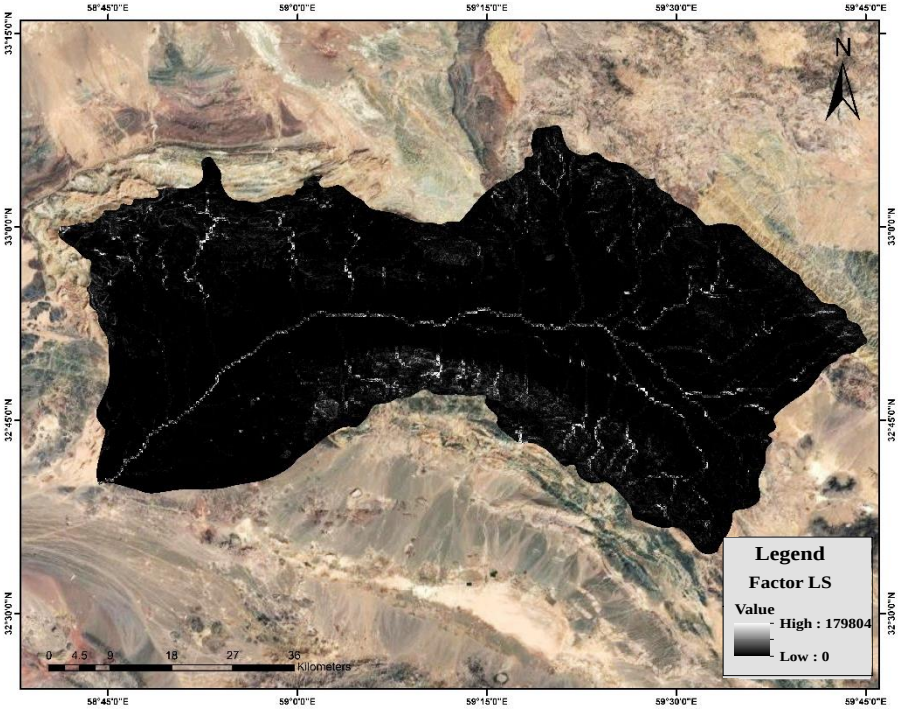

Fig. 7. Spatial distribution map of the slope length and steepness factor (LS) in the study area.

3.4. C factor

To calculate the C factor, vegetation cover data were first retrieved from the Google Earth Engine platform. As shown in Fig. 8, higher values indicate denser vegetation cover.

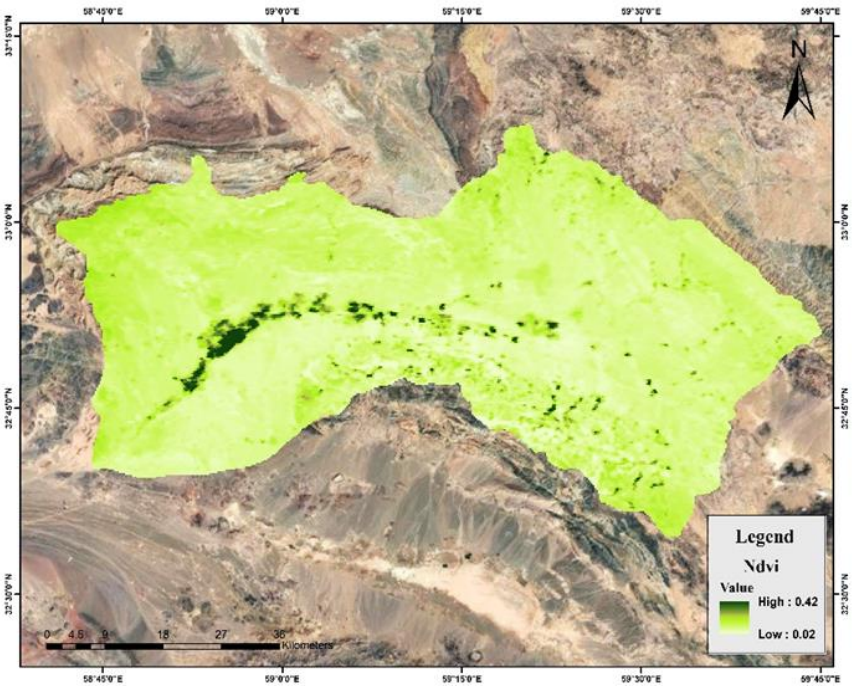

Fig. 8. Vegetation cover map of the Birjand plain, extracted from satellite imagery and processed in Google Earth Engine.

Subsequently, vegetation cover data were extracted from the Google Earth Engine platform and, using well-established empirical relationships, the computational code was developed within the Google Earth Engine environment to generate the C-factor map (Fig. 9). In this map, higher C-factor values indicate reduced vegetation density and quality, which correspond to increased soil erosion susceptibility. Conversely, lower C-factor values represent denser and more effective vegetation cover, which plays a significant role in reducing the impact energy of raindrops and surface runoff, thereby mitigating soil erosion rates.

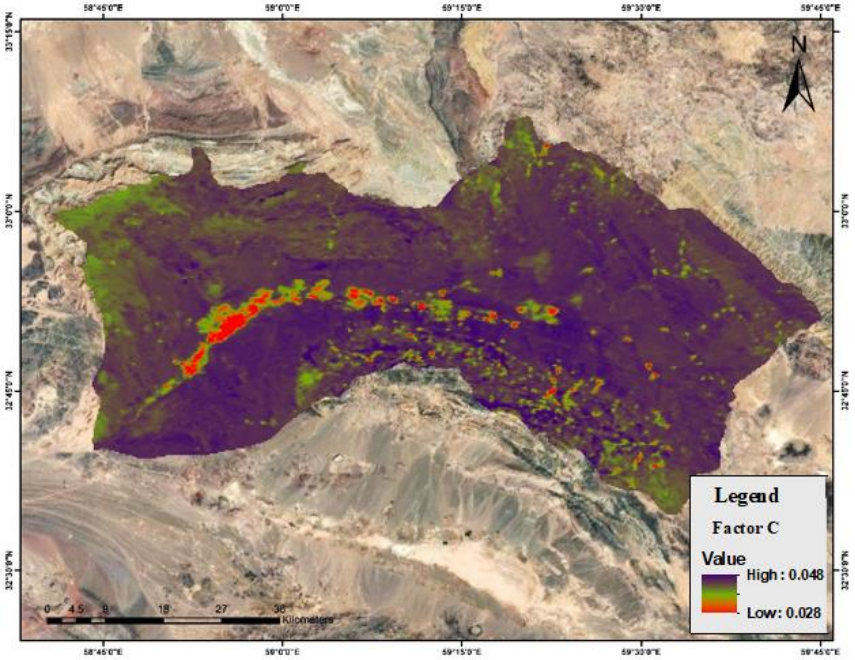

Fig. 9. Spatial distribution map of the Cover and Management Factor (C-factor) in the study area.

3.5. P factor

For the calculation of the P-factor, land use variables (Fig. 10) and slope (Fig. 6) were utilized, both of which were extracted as raster layers (images) through Google Earth Engine.

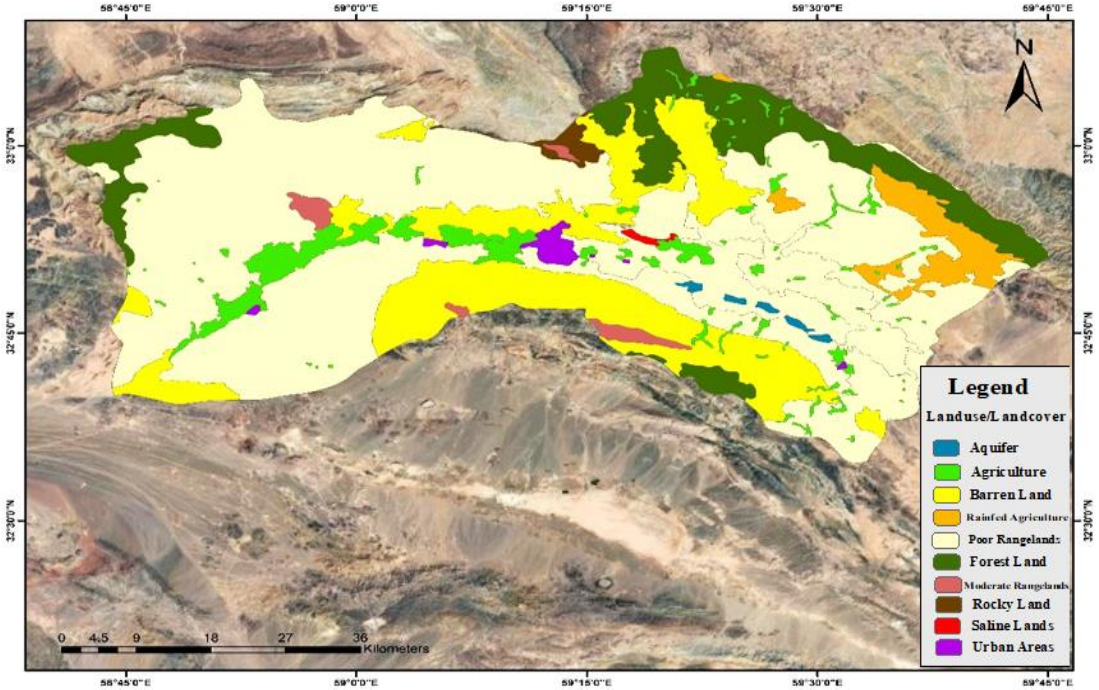

Fig. 10. Land use map of the study area, extracted from Google Earth data.

Subsequently, the P-factor was calculated using the standard equation. This factor is dimensionless and ranges between 0 and 1; lower values indicate better land management practices and higher effectiveness of conservation measures in reducing soil erosion (Fig. 11). Since detailed field data on conservation practices such as terracing or strip cropping were not available, the P-factor was approximated based on land use and slope classes, following commonly adopted approaches in similar remote sensing-based studies.

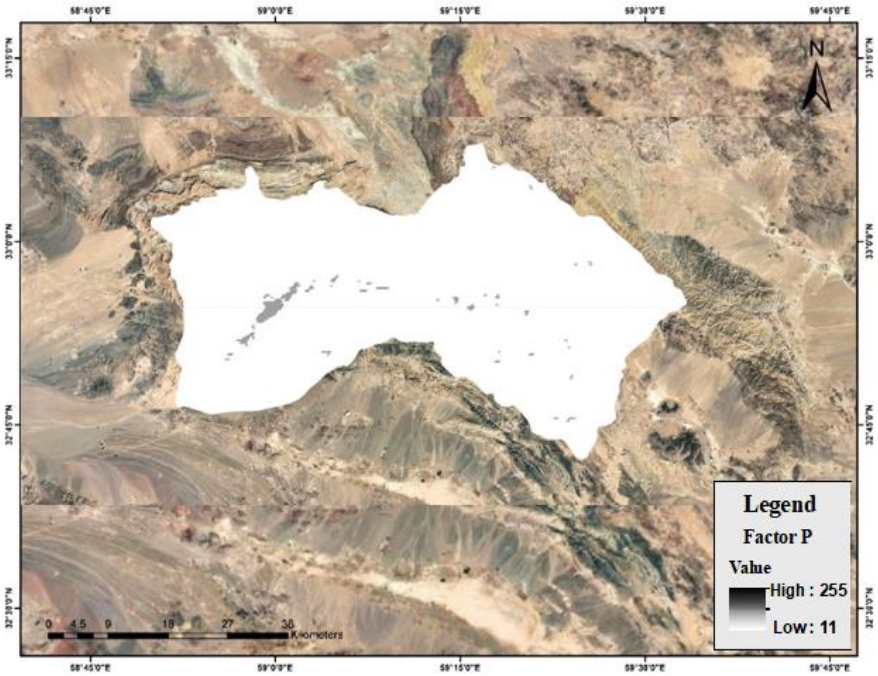

Fig. 11. Spatial distribution map of the conservation practice factor (P-factor) in the study area.

3.6. RUSLE Model

The Revised Universal Soil Loss Equation (RUSLE) model was applied in the Google Earth Engine environment by multiplying the R, K, LS, C, and P factors. This resulted in a spatially distributed soil erosion rate map. The estimated values range from 4 to 108.83 tons per hectare per year. Higher values indicate more intense erosion processes and greater soil vulnerability, especially in areas with insufficient vegetation cover or steep slopes, thus requiring urgent conservation and management interventions. Conversely, lower values suggest more stable conditions with reduced erosion risk. In the resulting RUSLE-based soil erosion map (Fig. 12), red-colored zones represent very high erosion severity, corresponding to areas of critical soil degradation. In contrast, green areas reflect minimal erosion and better soil conservation status. The classification of soil erosion severity across the Birjand Plain is summarized in Table 1, showing that:Very low erosion (0–10 t/ha/year) covers the majority of the area (67.32%), Followed by low (10–20 t/ha/year, 22.86%), Moderate (20–40 t/ha/year, 7.53%), High (40–60 t/ha/year, 2.03%), And very high erosion (60–108.83 t/ha/year) covering only 0.24% of the plain (Fig. 6).

Table 1. Classification of Average Annual Soil Loss in the Birjand Plain.

Name	Average Annual Soil Loss (tons per hectare per year)	Area (ha)	Percent (%)
Very Low	0-10	272762.5	67.32
Low	10-20	92618.75	22.86
Moderate	20-40	30500	7.53
High	40-60	8250	2.03
Very High	60-108/83	987.5	0.24

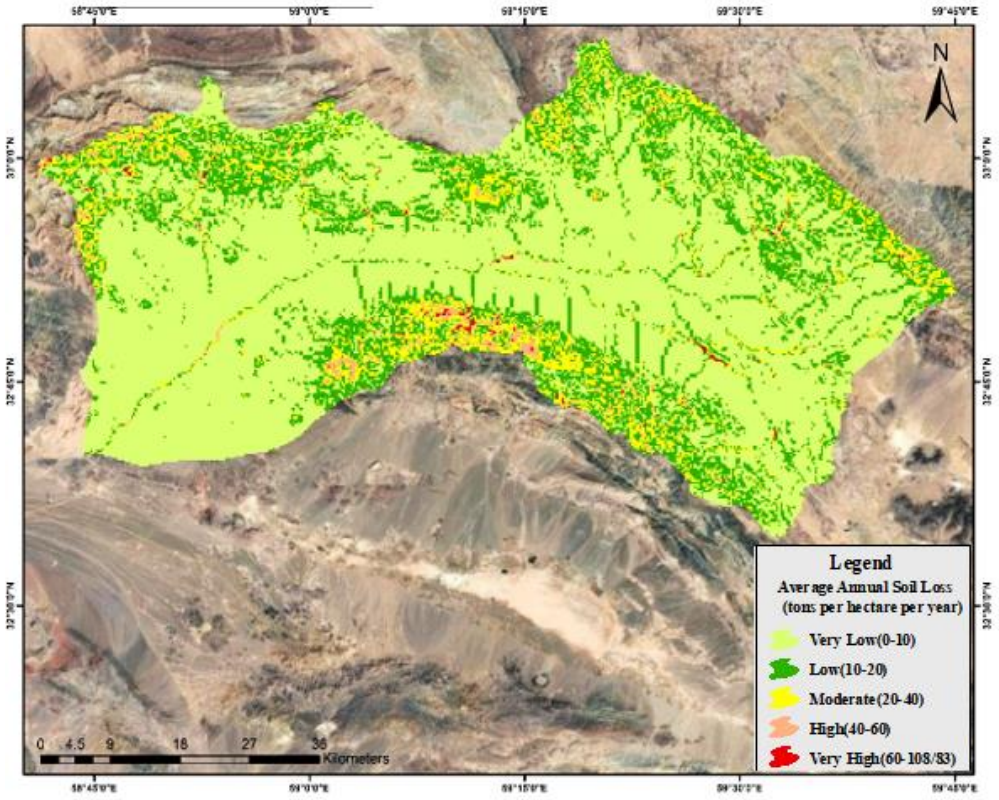

Fig. 12. Soil erosion estimation map using the RUSLE model in the study area.

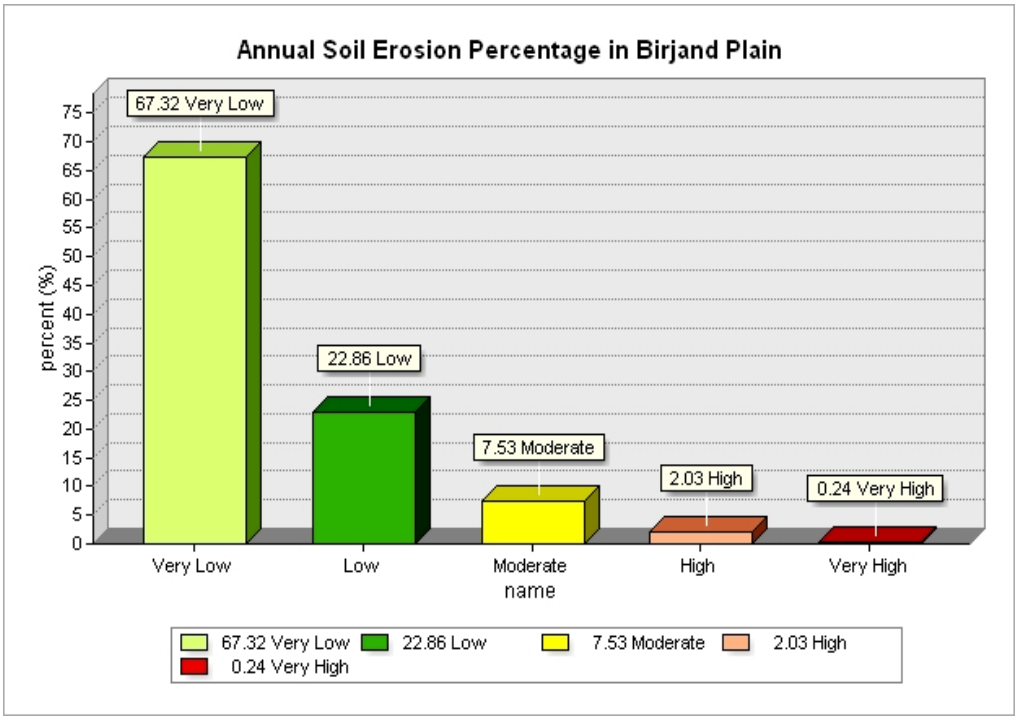

Fig. 6. Percentage of Soil Erosion Severity Classes in the Birjand Plain.

4. Conclusion

The present study demonstrated the successful integration of the RUSLE model with satellite data on the Google Earth Engine platform to estimate and spatially map soil erosion across the Birjand Plain. The analysis revealed that more than 90% of the area is subject to very low to low erosion risk (0–20 tons/ha/year), with only 2.2% falling under high to very high erosion classes (exceeding 40 tons/ha/year). These results point to a relatively stable soil condition in most of the plain, with

critical erosion concentrated in limited zones characterized by steep slopes, sparse vegetation, and suboptimal land management. When compared to similar studies across Iran, the Birjand Plain exhibits relatively lower erosion intensity. For instance, Ghahremani et al. (2025) reported an average erosion of 18.82 tons/ha/year even after biological conservation interventions in the Chikan and Morzian basins. Gholami et al. (2024) observed a sharp increase from 13.23 to 20.13 tons/ha/year due to land use changes in Cherdawol, while Garshasbi and Jokar (2024) recorded an increase in erosion from 1.64 to 1.75 tons/ha/year following deforestation in Avard-Nakarood. Asghari and Babaei (2024) also noted increased erosion in Shafarood due to urban expansion, with values rising from 5.63 to 8.37 tons/ha/year. In contrast, the majority of the Birjand Plain exhibits annual erosion rates below 20 tons/ha/year, indicating relatively favorable topographic and land cover conditions across much of the region. Furthermore, this study highlights the efficiency of cloud-based approaches in erosion modeling. While Jokar Sarhangi and Dehghan Chachkami (2022) evaluated model accuracy by comparing RUSLE with ICONA, and Terefe et al. (2024) explored RUSLE's application in Ethiopia, the present work confirms that—when fed with reliable satellite inputs—RUSLE remains a robust and adaptable framework for soil erosion assessment across diverse landscapes. The use of GEE not only accelerates analysis but also ensures reproducibility and scalability, making it suitable for continuous monitoring and management planning. In light of the identified critical erosion zones—primarily located on steep slopes with limited vegetation—implementing targeted conservation practices is recommended. These may include contour plowing, vegetative buffer strips, terracing, and afforestation using drought-resistant species. In addition, promoting sustainable land use planning and farmer education programs can enhance the adoption of soil-friendly practices. Scenario-based modeling of these interventions in future research may also help evaluate their long-term impact on erosion mitigation and land productivity. Future studies are encouraged to incorporate higher-resolution and field-validated datasets, especially for soil and land management parameters. Integrating machine learning techniques with GEE could further enhance the prediction accuracy and automation of erosion modeling. Additionally, linking RUSLE results with socio-economic and land tenure data could improve policy-relevant insights for sustainable land management and erosion mitigation strategies. Given the increasing frequency of extreme rainfall events in arid and semi-arid regions, future research is recommended to incorporate climate change scenarios into the estimation of the R-factor. Moreover, integrating soil erosion outputs with hydrological models such as SWAT can help assess the downstream impacts of erosion on water quality. Additionally, future studies are encouraged to evaluate the socio-economic implications of soil erosion, particularly its impacts on agricultural productivity, land value, and livelihoods of local farmers. Integrating land ownership and usage patterns may also support more effective, community-based soil conservation strategies.

Acknowledgments

This article was not under any financial support.

References

Alewell, C., Borrelli, P., Meusburger, K. & Panagos, P., 2019. Using the USLE: Chances, challenges and limitations of soil erosion modelling. *International Soil and Water Conservation Research*, 7(3), 203-225.

Almagro, A., Thomé, T.C., Colman, C.B., Pereira, R.B., Marcato Junior, J., Rodrigues, D.B.B. & Oliveira, P.T.S., 2019. Improving cover and management factor (C-factor) estimation using remote sensing approaches for tropical regions. *International Soil and Water Conservation Research*, 7(4), 325-334.

Asadi, H., Honarmand, M., Vazifedoust, M. & Moussavi, A., 2017. Assessment of changes in soil erosion risk using RUSLE in Navrood watershed, Iran. *Journal of Agricultural Science and Technology*, 19(1), 231-244.

Asghari Saraskanroud, S. & Babaei Olam, T., 2024. Evaluation of the impact of land use changes over a twenty-year period on soil erosion in the Shafarood watershed using the RUSLE model. *Journal of Environmental Science Studies*, 9(2), 8516-8530.

Belnap, J., Munson, S. & Field, J., 2011. Aeolian and fluvial processes in dryland regions: The need for integrated studies. *Ecohydrology*, 4(5), 615-622.

Biddoccu, M., Guzmán, G., Capello, G., Thielke, T., Strauss, P., Winter, S., Zaller, J.G., Nicolai, A., Cluzeau, D., Popescu, D., Bunea, C.,

Hoble, A., Cavallo, E. & Gómez, J.A., 2020. Evaluation of soil erosion risk and identification of soil cover and management factor (C) for RUSLE in European vineyards with different soil management. *International Soil and Water Conservation Research*, 8(4), 337-353.

Boardman, J., 2006. Soil erosion science: Reflections on the limitations of current approaches. *Catena*, 68(2-3), 73-86.

Chuenchum, P., Xu, M. & Tang, W., 2020. Estimation of soil erosion and sediment yield in the Lancang-Mekong River using the Modified revised universal soil loss equation and GIS techniques. *Water*, 12(1), 135.

De Jong, S., Paracchini, M., Bertolo, F., Folving, S., Megier, J. & De Roo, A., 1999. Regional assessment of soil erosion using the distributed model SEMMED and remotely sensed data. *Catena*, 37(3), 291-308.

Duan, X., Bai, Z., Rong, L., Li, Y., Ding, J., Tao, Y., Li, J., Li, J. & Wang, W., 2020. Investigation method for regional soil erosion based on the Chinese Soil Loss Equation and high-resolution spatial data: Case study on the mountainous Yunnan Province, China. *Catena*, 184, 104237.

Ebrahimzadeh, S., Motagh, M., Mahboub, V. & Harijani, F. M., 2018. An improved RUSLE/SDR model for the evaluation of soil erosion. *Environmental Earth Sciences*, 77(12), 1-17.

Farhan, Y. & Nawaiseh, S., 2015. Spatial assessment of soil erosion risk using RUSLE and GIS techniques. *Environmental Earth Sciences*, 74(6), 4649-4669. https://doi.org/10.1007/s12665-015-4430-7

Gholami, L., Khaledi Darvishan, A., Derakhti, S. & Kiani Harchegani, M., 2024. Effects evaluation of land use change on soil erosion using the RUSLE model in the Chardavol watershed, Ilam. *Journal of Watershed Management Science and Engineering*, 18(65), 1.

Guerra, C.A., Maes, J., Geijzendorffer, I. & Metzger, M. J., 2016. An assessment of soil erosion prevention by vegetation in Mediterranean Europe: Current trends of ecosystem service provision. *Ecological Indicators*, 60, 213-222.

Jokar Sarhangi, E. & Dehghan Chachkami, M.R., 2022. Evaluation of the efficiency of RUSLE and ICONA models in soil erosion zoning of the Baldeh watershed, Mazandaran province. *Journal of Natural Environmental Hazards*, 11(34), 159-178.

Kebede, B., Tsunekawa, A., Haregeweyn, N., Adgo, E., Ebabu, K., Meshesha, D.T., Tsubo, M., Masunaga, T. & Fenta, A. A., 2020. Determining C-and Ps of RUSLE for different land uses and management practices across agro-ecologies: Case studies from the Upper Blue Nile basin, Ethiopia. *Physical Geography*, 1-23.

Le Roux, J.J., Morgenthal, T.L., Malherbe, J., Pretorius, D.J. & Sumner, P. D., 2008. Water erosion prediction at a national scale for South Africa. *Water SA*, 34(3), 305-314.

Liu, B.Y., Nearing, M.A. & Risse, L.M., 1994. Slope gradient effects on soil loss for steep slopes. *Transactions of the ASAE*, 37(6), 1835-1840.

McCool, D.K., 1985. Crop residue effects on erosion from dry-farmed cropland in the Pacific Northwest (Paper No. 85-2046). American Society of Agricultural Engineers.

Mitasova, H., Hofierka, J., Zlocha, M. & Iverson, L. R., 1996. Modelling topographic potential for erosion and deposition using GIS. *International Journal of Geographical Information Systems*, 10(5), 629-641.

Moore, I.D. & Wilson, J.P., 1992. Length-slope factors for the revised universal soil loss equation: Simplified method of estimation. *Journal of Soil and Water Conservation*, 47(5), 423-428.

Natural Capital Project, (n.d.). Natural Capital Project. Stanford University. Retrieved March 27, 2022, from

Neitsch, S.L., Arnold, J.G., Kiniry, J.R. & Williams, J.R., 2011. Soil and Water Assessment Tool theoretical documentation version 2009. Texas Water Resources Institute.

Owens, P.N. & Collins, A.J., 2006., Soil erosion and sediment redistribution in river catchments: Measurement, modelling and management. CABI.

Panagos, P., Borrelli, P., Poesen, J., Ballabio, C., Lugato, E., Meusburger, K., Montanarella, L. & Alewell, C., 2010. The new assessment of soil loss by erosion index. *Journal of Watershed Management Researches*, 89, 44-51.

Pimentel, D., 2006. Soil erosion: A Food and environmental threat. *Environment, Development and Sustainability*, 8(1), 119-137.

Rahimzadeh Kivi, M., Hamzeh, S. & Kardan Moghaddam, H., 2015. Determining groundwater quality vulnerability in Birjand plain using the DRASTIC model and its calibration by AHP method. *Journal of Physical Geography Research*, 47(3), 25-38.

Robinson, D.A., Panagos, P., Borrelli, P., Jones, A., Montanarella, L., Tye, A. & Obst, C.G., 2017. Soil natural capital in Europe; a framework for state and change assessment. *Scientific Reports*, 7(1), 6706.

Rostamian, R., Jaleh, A., Afyuni, M., Mousavi, S. F., Heidarpour, M., Jalalian, A. &

Abbaspour, K. C., 2008. Application of SWAT model for estimating runoff and sediment in two mountainous basins in central Iran. *Hydrological Sciences Journal*, 53(5), 977-988.

Samarinas, N., Tsakiridis, N.L., Kalopesa, E. & Zalidis, G.C., 2024. Soil loss estimation by water erosion in agricultural areas: Introducing artificial intelligence geospatial layers into the RUSLE model. *Land*, 13(2), 174.

Tamene, L., Adimassu, Z., Aynekulu, E. & Yaekob, T., 2017. Estimating landscape susceptibility to soil erosion using a GIS-based approach in Northern Ethiopia. *International Soil and Water Conservation Research*, 5(3), 221-230.

Terefe, B., Melese, T., Tsegaye, A., Afework, A., Yibeltal, T., Anagaw, A., Temesgen, F., Belay, T., Assefa, G. & Mencho, B. B., 2024. Application of RUSLE model for soil loss estimation in Ethiopia: A systematic review of strengths, limitations, and future directions. *Environmental Monitoring and Assessment*, 196(2), 794.

Walker, B. & Steffen, W., 1997. An overview of the implications of global change for natural and managed terrestrial ecosystems. *Conservation Ecology*, 1(2), 16.

Wang, Z. & Su, Y., 2020. Assessment of soil erosion in the Qinba mountains of the southern Shaanxi Province in China using the RUSLE model. *Sustainability*, 12(5), 1733.

Weiner, F.F., 1981. Treatment of phonological disability usng the method of meaningful minimal contrast: Two case studies. *Journal of Speech and Hearing Disorders*, 46(1), 97-103.

Wischmeier, W.H. & Smith, D.D., 1978. Predicting rainfall ersion losses: A guide to conservation planning (Agriculture Handbook No. 537, p. 58). U.S. Department of Agriculture.

Xu, S., Liu, Y., Gong, J., Wang, C. & Wang, Z., 2020. Coparing differences among three ecosystem service proxies for soil erosion prevention and their combination characteristics at local scales. *Ecological Indicators*, 110, 105929.